OXFORD

*Cerebral Cortex*, 2023, **33**, 9756–9763
https://doi.org/10.1093/cercor/bhad241
Advance access publication date 6 July 2023
Original Article

# Relating white matter microstructure in theoretically defined addiction networks to relapse in alcohol use disorder

Donovan J. Roediger[1], Claire Griffin[2], Frances V. Marin[3], Hannah Verdoorn[1], Mark Fiecas[4], Bryon A. Mueller[1], Kelvin O. Lim[1], Jazmin Camchong[1,*]

[1]Department of Psychiatry and Behavioral Sciences, University of Minnesota, Minneapolis, MN 55455, United States,
[2]Berenson-Allen Center for Noninvasive Brain Stimulation, Beth Israel Deaconess Medical Center, Boston, MA 02215, United States,
[3]Center for Mindfulness and Compassion, Cambridge Health Alliance, Cambridge, MA 02141, United States,
[4]Division of Biostatistics, School of Public Health, University of Minnesota, Minneapolis, MN 55455, United States

*Corresponding author: Department of Psychiatry and Behavioral Sciences, University of Minnesota; 2450 Riverside Ave., F253, Minneapolis, MN 55454, United States. Email: camch002@umn.edu

Theoretical models group maladaptive behaviors in addiction into neurocognitive domains such as incentive salience (IS), negative emotionality (NE), and executive functioning (EF). Alterations in these domains lead to relapse in alcohol use disorder (AUD). We examine whether microstructural measures in the white matter pathways supporting these domains are associated with relapse in AUD. Diffusion kurtosis imaging data were collected from 53 individuals with AUD during early abstinence. We used probabilistic tractography to delineate the fornix (IS), uncinate fasciculus (NE), and anterior thalamic radiation (EF) in each participant and extracted mean fractional anisotropy (FA) and kurtosis fractional anisotropy (KFA) within each tract. Binary (abstained vs. relapsed) and continuous (number of days abstinent) relapse measures were collected over a 4-month period. Across tracts, anisotropy measures were typically (i) lower in those that relapsed during the follow-up period and (ii) positively associated with the duration of sustained abstinence during the follow-up period. However, only KFA in the right fornix reached significance in our sample. The association between microstructural measures in these fiber tracts and treatment outcome in a small sample highlights the potential utility of the three-factor model of addiction and the role of white matter alterations in AUD.

*Key words*: alcohol use disorder; diffusion MRI; relapse; white matter.

## Introduction

Alcohol use disorder (AUD) is a common psychiatric condition characterized by chronic alcohol use despite harmful consequences. In the United States, roughly 30% of adults will meet criteria for AUD at some point in their lives (Grant et al. 2015). Although residential and outpatient treatment programs are widely available, patients with AUD frequently relapse following treatment and are trapped in a cycle between treatment, abstinence, and relapse (McKay and Hiller-Sturmhöfel 2011). AUD's persistent relapse rates highlight the importance of developing new treatment strategies such as neuromodulation interventions that are designed with a greater understanding of the risk factors and neurobiological mechanisms involved in relapse.

AUD results from a culmination of psychosocial, environmental and biological factors (Deeken et al. 2020; Ossola et al. 2021). Among the biological factors are maladaptive alterations to neurocircuitry, which have been a primary focus of addiction research for the past several decades. Koob and Volkow synthesized this body of animal and human imaging research into a theoretical model which describes the neural pathophysiology of addiction (Koob and Volkow 2010; Koob and Volkow 2016). This framework outlines three neurofunctional domains impacted in addiction: incentive salience (IS; e.g. exaggerated reward response from a drug), negative emotionality (NE; e.g. withdrawal and exaggerated stress when not using), and executive functioning (EF; e.g. preoccupation with a substance; heightened impulsivity).

The neurofunctional domains identified by Koob and Volkow and alterations to the structures that underlie those domains may explain individual variation in resilience to relapse (Koob and Volkow 2010; Koob and Volkow 2016). We previously showed that reduced resting state functional connectivity measured during early abstinence within addiction networks defined by Koob and Volkow's theoretical model of addiction were associated with an increased risk of relapse and predicted days-to-relapse in AUD (Camchong et al. 2022). In the present manuscript, we leverage modern diffusion MRI techniques to examine white matter microstructure within white matter tracts connecting regions within these addiction networks. For each of the three Koob–Volkow domains, we identified a white matter tract based on prior research. Fig. 1 illustrates these three tracts in an example participant.

### IS domain and the fornix

In AUD, the IS domain involves an exaggerated reward response to alcohol. This heightened reward response is thought to be

**Received:** January 23, 2023. **Revised:** June 5, 2023. **Accepted:** June 7, 2023

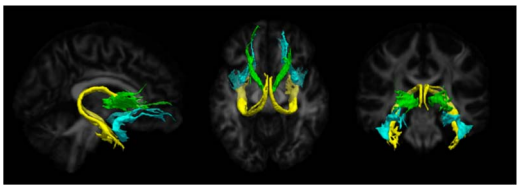

**Fig. 1.** Tractography results rendered as 3D surfaces overlaid on an FA map. The fornix (yellow), uncinate fasciculus (blue), and anterior thalamic radiations (green) correspond to the IS, NE, and EF domains, respectively.

modulated by excess dopaminergic activity in the mesolimbic reward pathway (Vollstädt-Klein et al. 2010; Sanchez-Roige et al. 2014), including the nucleus accumbens. Supporting connectivity between the nucleus accumbens and several other limbic structures (e.g. hippocampus, thalamus, and hypothalamus), the fornix is a primary white matter pathway mediating reward and memory circuitry (Brown and Winocur 1973; Shin et al. 2019). Decreased FA in the fornix has been reported in alcoholics relative to controls (Pfefferbaum et al. 2009) and fornix FA has been shown to be negatively correlated with alcohol cue reactivity in heavy drinkers (Monnig et al. 2013).

### NE domain and the uncinate fasciculus

The NE domain describes how alcohol-seeking behavior in AUD is characterized by negative affect such as dysphoria, anxiety, and withdrawal symptoms when access to alcohol is limited. These negative emotional responses have been shown to be primarily mediated by the release of corticotropin releasing factor in the extended amygdala (Koob and Volkow 2010). The uncinate fasciculus (UF) is a hook-shaped white matter tract joining the amygdala and orbitofrontal cortex. This tract is thought to play a key role in emotional responses to events and has been implicated in disorders involving emotional regulation (e.g. anxiety disorders, depression, and conduct disorder) (Taylor et al. 2007; Olson et al. 2015; Damme et al. 2017). UF diffusivity has been shown to be related to levels of anxiety and depression in individuals with heroin addiction (Wong et al. 2015). Microstructural changes in UF have been reported in adolescent cigarette smokers (Zhou et al. 2022) and adolescent binge alcohol drinkers (Jacobus et al. 2013; Luciana et al. 2013).

### EF domain and the anterior thalamic radiation

In AUD, the EF domain involves impaired impulse control and persistent and habitual alcohol-seeking behavior despite the desire to avoid negative consequences of alcohol use. The top-down executive control functions affected in AUD are primarily mediated by the prefrontal cortex (Goldstein and Volkow 2011), working in conjunction with thalamic, cerebellar, and parietal cortices (Dosenbach et al. 2008). The anterior thalamic radiation is a major thalamocortical projection between the dorsolateral prefrontal cortex and the dorsomedial thalamic nucleus through the internal capsule's anterior limb and is known to be involved in EF (Mamiya et al. 2018; Niida et al. 2018; Haddad et al. 2021). Studies have linked alterations in ATR microstructure with heightened impulsivity (Joutsa et al. 2011; Yuan et al. 2017; Alfano et al. 2021). Recent evidence suggests that substance use disorders may be associated with decreased ATR volume (Pando-Naude et al. 2021).

### White matter microstructure metrics

We assessed white matter microstructure in each of the three pathways using diffusion kurtosis imaging (DKI), a framework for modeling the diffusion signal that improves upon the standard tensor model by accounting for deviations from Gaussianity (Jensen and Helpern 2010). We focused on anisotropy of both the diffusion tensor (fractional anisotropy, FA) and kurtosis tensor (kurtosis fractional anisotropy, KFA). These metrics range from 0 to 1, where 0 represents perfect isotropy and 1 represents complete directional cohesion along the primary axis.

FA was chosen as the primary metric of interest due to its widespread clinical and research use, allowing for easier comparisons to prior research. KFA was also examined because it has been shown to offer supplementary information and improved contrast in complex tissues and deep brain structures where FA often approaches zero (Hansen and Jespersen 2016). We and others have hypothesized that KFA's enhanced ability to distinguish various microstructural compositions of white matter results in an improvement over FA in diagnostic sensitivity (Hansen and Jespersen 2016; Hansen 2019; Zhang et al. 2019). By including both metrics, we aimed to leverage the more advanced kurtosis model while maintaining the ability to compare our results to prior studies which used the standard tensor model.

To determine whether white matter microstructure is associated with subsequent relapse outcome, we investigated here whether FA and KFA metrics within these three tracts (a) predict dichotomous relapse (relapsed vs. abstained) during a 4-month follow-up period and (b) predict the number of days until relapse during a 4-month follow-up period.

## Methods

### Participants

Participants with AUD were recruited 1–2 weeks following admission to a 28-day in-patient addiction treatment program in Minneapolis, MN as part of a longitudinal study. This analysis focuses on imaging data collected during early abstinence (mean number of days abstinent until MRI session = 25.4, SD = 13.2) and relapse data collected at a four month follow up interview. Written informed consent was obtained from each participant. Participants received monetary compensation for their time. The Institutional Review Board at the University of Minnesota reviewed and approved the consent process and all study procedures. The data that support the findings of this study are available from the corresponding author upon reasonable request.

A total of 86 participants were consented. From these, 11 did not complete the MRI session for the following reasons: 3 left the treatment program and were no longer reachable before the MRI session, 3 participants opted out of the study after consent and before the MRI session, and 5 were found to be no longer eligible (3 because of medical conditions, 1 because of unknown metal in body, and 1 because it was discovered that the identified *primary* substance use disorder diagnosis was not alcohol, but methamphetamine). Of the 75 participants who completed an MRI session, 6 were missing diffusion MRI data due to time constraints during the MRI session. Of the 69 participants from whom we collected diffusion MRI data, 16 were lost to follow-up after the MRI session. As a result, complete data for the scope of this paper (neuroimaging and treatment outcome data) were available for 53 individuals with AUD (Table 1).

Participants underwent random alcohol and drug tests in the treatment program. Each participant's substance use history for the past 6 months before entering the treatment program was recorded using the Timeline Follow-Back (TLFB) (Sobell and Sobell 1992) assessment that was administered for alcohol and for each other substance used (excluding caffeine) (Table 1).

**Table 1.** Demographics, history of alcohol use, and clinical self-report measures in individuals with AUD during early abstinence.

| | | Sample separated by treatment outcome at 4-month follow-up | | |
|---|---|---|---|---|
| Characteristic | All AUD ($n = 53$)<br>Mean *or* *n* (SD *or* %) | ABS ($n = 27$)<br>Mean *or* *n* (SD *or* %) | REL ($n = 26$)<br>Mean *or* *n* (SD *or* %) | ABS vs. REL<br>*P*-value for t-test or $\chi^2$ *(italics)* |
| Age | 42.8 (10.1) | 44.1 (10.8) | 41.3 (9.3) | $P = 0.32$ |
| Years of education | 14.2 (2.1) | 14.3 (2.0) | 14.1 (2.2) | $P = 0.66$ |
| Female, *n* % | 19 (35.9%) | 6 (22.2%) | 13 (50.0%) | $P = 0.09$ |
| Employed, *n* % | 21 (39.6%) | 12 (44.4%) | 9 (34.6%) | $P = 0.57$ |
| Age of AUD onset | 24.7 (10.7) | 25.2 (10.8) | 24.1 (10.6) | $P = 0.70$ |
| # of standard drinks: past 6 months | 2,799.2 (2,226.8) | 2,538.8 (1,876.9) | 3,069.5 (2,549.7) | $P = 0.39$ |
| # drinking days: past 6 months | 101.7 (58.1) | 101.8 (58.6) | 99.5 (58.7) | $P = 0.89$ |
| # days abstinent before MRI session | 22.4 (13.2) | 23.5 (10.7) | 21.3 (15.5) | $P = 0.55$ |
| Beck Depression Inventory (BDI)[a] | 21.6 (12.0) | 21.6 (13.2) | 21.7 (10.9) | $P = 0.97$ |
| State Anxiety Inventory (STAI)[a] | 42.2 (11.2) | 39.7 (12.0) | 44.5 (10.1) | $P = 0.12$ |
| Penn Alcohol Craving Scale (PACS)[a] | 21.9 (7.4) | 21.5 (8.4) | 22.3 (6.4) | $P = 0.71$ |

AUD, alcohol use disorder; MRI, magnetic resonance imaging; SD, standard deviation; ABS, those that remained abstinent in the 4-month follow-up period; REL, those that relapsed during the 4-month follow-up period; $\chi^2$, chi-square; *p*, significance probability value. [a]One participant (ABS) did not complete any self-report measures. Four participants (two REL, two ABS) completed PACS and BDI, but not STAI.

Study participants completed clinical self-report measures that have been associated with relapse (Oliva et al. 2018; Stohs et al. 2019; Pareaud et al. 2021) (Table 1): the Beck Depression Inventory (BDI; Beck et al. 1988); the State Anxiety Inventory (STAI; Spielberger et al. 1970); and the Penn Alcohol Craving Scale (PACS; Flannery et al. 1999). Participants completed interviews during a 4-month follow-up period after the neuroimaging session to query dichotomous and continuous relapse metrics.

### *Dichotomous relapse metrics: group definition*

Participants were considered to be in the relapsing group (REL) if they reported consuming at least one drink and/or non-prescribed drug during the 4-month follow-up period. Participants who reported consuming no alcohol or non-prescribed drug during the 4-month follow-up period were considered to be in the abstaining group (ABS).

### *Continuous relapse metrics*

Detailed TLFB (Sobell and Sobell 1992) data were collected from the REL group, recording date of relapse, number of drinks, and number of drinking days after relapse during the 4-month follow-up period. Time to relapse to alcohol use was operationalized as the number of days until a participant's self-reported first use of alcohol. The variable representing the number of drinks (standard drink, equivalent to 0.6 ounces of pure alcohol (Alcohol Questions and Answers | CDC 2022) after relapse was operationalized as the number of drinks reported to have been consumed in the 4-month follow-up period. The number of days drinking was operationalized as the number of days reported to have consumed at least one drink during the 4-month follow-up period (Table 1).

## Imaging data acquisition and analysis

MRI data were collected using a 3 T Siemens Prisma scanner (Siemens, Erlangen, Germany) at the University of Minnesota Center for Magnetic Resonance Research. Acquired images included: a T1-weighted MPRAGE image [TR = 2,400 ms, TE = 2.24 ms, slices = 208, voxel size = 0.8 $mm^3$], a T2-weighted SPACE image [TR = 3,200 ms, TE = 564 ms, slices = 208, voxel size = 0.8 $mm^3$], and a pair of multi-shell diffusion-weighted images collected using reversed phase-encode blips [TR = 3,100 ms, TE = 85 ms, slices = 92, voxel size = 1.5 $mm^3$, multi-band factor = 4, *b* values of 0, 1,000, and 2,000 $s/mm^2$].

Image data were preprocessed using the HCP minimal preprocessing pipelines (v4.0.1) (Glasser et al. 2013). For structural data, these steps included alignment of the T1-weighted volume to the T2-weighted volume, correction for gradient distortion and intensity bias, volume segmentation and surface reconstruction using FreeSurfer (v6.0.0) (Dale et al. 1999) and calculation of nonlinear transforms to standard MNI152 space. Diffusion preprocessing included rigid AC-PC alignment to the native structural images, correcting for susceptibility-related distortions using the "topup" tool from the Functional Magnetic Resonance Imaging of the Brain Software Library (FSL; Andersson et al. 2003; Smith et al. 2004), and eddy current distortion with slice outlier replacement using FSL's "eddy" tool (Andersson et al. 2016; Andersson and Sotiropoulos 2016; Andersson et al. 2017; Andersson et al. 2018).

Tractography was carried out using FSL's XTRACT (Warrington et al. 2020), in which expertly defined masks in MNI152 space are warped to native space and used to guide probabilistic tractography of a set of 42 major white matter pathways (19 bilateral and 4 commissural) in each participant, including the 6 tracts of interest (3 bilateral) examined in the present study (Table 2). Tracts of interest were then visually inspected by an experienced rater (D.J.R.) to ensure they were free from anomalies or discernible processing errors. Finally, we refined each tract of interest by excluding voxels with less than 20% of the robust maximum probability of tract membership.

White matter microstructure in each tract was assessed using FA and KFA metrics. FA is a frequently used measure of the anisotropy of the diffusion signal when the tensor model is applied to the data, while KFA reflects the anisotropy of the non-gaussian component (kurtosis tensor) when the higher order kurtosis model is applied to the diffusion signal (Glenn et al. 2015). KFA provides superior contrast in complex tissues compared to standard diffusion tensor models (Hansen and Jespersen 2016). Whole brain FA and KFA scalar maps were calculated from the preprocessed diffusion images using the Diffusion Kurtosis Estimator package (Tabesh et al. 2011). Average tract-wise values were then calculated for each tract, weighted by voxel-wise likelihood of tract membership.

## Statistical analysis

First, to determine whether there were significant demographic differences on dichotomous relapse metrics (ABS vs. REL defined

**Table 2.** Koob–Volkow addiction domains and underlying brain regions and associated white matter pathways.

| Domain | Description | Brain Regions (Koob and Volkow 2016; Kwako et al. 2019) | Proposed associated white matter pathway |
|---|---|---|---|
| Reward and Incentive salience (IS) | Exaggerated dopaminergic reward response | Nucleus accumbens<br>Caudate<br>Putamen<br>Globus pallidum<br>Thalamus | Fornix (Fx) |
| Negative emotionality (NE) | Withdrawal and exaggerated stress when not using | Amygdala<br>Caudate<br>Habenula<br>Nucleus accumbens | Uncinate fasciculus (UF) |
| Executive functioning (EF) | Preoccupation with drug; heightened impulsivity | Prefrontal cortex<br>Orbitofrontal cortex<br>Hippocampus<br>insula | Anterior thalamic radiation (ATR) |

For each white matter pathway, left and right hemispheres were examined separately.

at the 4-month follow-up period), independent samples t-test were conducted on age, years of education, clinical self-report measures (i.e. BDI, STAI, PACS, SCQ), and substance use history (age of onset of alcohol dependence, number of drinks in the past 6 months, number of days drinking in the past 6 months, number of days abstinent until MRI data collection day). To determine whether there were sex (as a biological variable) differences between groups (REL vs ABS), Pearson's chi-square tests were conducted (Table 1).

Binary logistic regression models were fit to assess whether FA and KFA in our tracts-of-interest predicted binary outcome (REL vs ABS) at a 4-month follow-up. Cox proportional hazards models were used to assess whether FA and KFA in our tracts-of-interest predicted days-to-relapse. For these models, anisotropy metrics were linearly scaled by a factor of 100 to facilitate the interpretability of the coefficient estimates. Each tract-of-interest in each hemisphere was modeled separately and separate analyses were conducted for KFA and FA. Based on the total number of tracts examined (6), a Bonferroni-adjusted significance threshold of 0.0083 was used.

## Results

No demographic differences were found between REL and ABS groups (Table 1), Despite there being no significant relationship between sex and age and either continuous or binary relapse measures in our sample, we adjusted for these variables in each model to account for observed trend-level relationships and prior reports of potential effects (Sliedrecht et al. 2019). No significant differences were found in any self-report measures between REL and ABS groups (Table 1).

### Diffusion metrics and risk of relapse

#### *Dichotomous relapse metric*

Descriptive statistics for tract-wise FA and KFA measurements are reported in Table 3. After correcting for the number of comparisons within each diffusion metric by using a Bonferroni-adjusted alpha ($\alpha = 0.0083$), only KFA in the right fornix was a significant predictor ($P = 0.006$) of dichotomous relapse in sex and age-adjusted binary logistic regression models (Table 4); FA in this tract did not survive correction for multiple comparisons ($P = 0.018$). Results in the bilateral UF suggest that a negative relationship between anisotropy measures and dichotomous relapse may be uncovered in a larger sample, but these did not reach significance in our sample.

#### *Continuous relapse metric*

Results of the sex and age-adjusted Cox regression models predicting the number of days to relapse (see Table 5) bore similarities to the logistic regression models predicting dichotomous relapse reported above. In the right fornix, KFA significantly predicted the number of days until relapse ($P = 0.002$), with increased KFA associated with longer periods of abstinence. FA in this tract showed a similar relationship but did not survive Bonferroni correction ($P = 0.011$). In the bilateral UF, the relationship between anisotropy measures and abstinence duration was in the same direction as observed in the right fornix but failed to reach significance.

## Discussion

This study follows a previous report in which we leveraged the same theory-driven addiction model (Koob and Volkow 2016; Kwako et al. 2019) to examine whether resting state functional connectivity (RSFC) within each addiction domain was associated with binary and continuous relapse metrics (Camchong et al. 2022). This study expands on our brain functional connectivity work by examining whether white matter microstructural alterations in tracts within those same theoretical addiction domains are also predictive of subsequent relapse outcomes (as dichotomous and continuous variables). By examining anatomical metrics that are relatively stable across time, we hoped to both address reliability concerns inherent in RSFC analyses (Noble et al. 2019) and explore potential structural explanations for previously observed RSFC hypoconnectivity.

We examined three pairs of contralateral tracts representing the three addiction domains (Table 2) using two diffusion-based metrics (FA and KFA) that are sensitive to microstructural alterations in white matter. Our approach revealed a relationship between white matter microstructure in one tract associated with the IS domain (right fornix) and non-significant effects in the same direction in the NE domain (bilateral UF). There was no apparent relationship between white matter microstructure and the bilateral ATR, which was selected as representative of the EF domain.

KFA in the right fornix (IS domain) was significantly associated with both dichotomous (relapsed: yes vs. no) and continuous (number of days to relapse) relapse metrics during the 4-month follow-up period, after controlling for age and sex and after correction for multiple comparisons. The IS domain was the

**Table 3.** Descriptive statistics of tract-wise FA and KFA measurements.

| | | | *All AUD* | | *ABS* | | *REL* | |
|---|---|---|---|---|---|---|---|---|
| *Domain* | *Tract* | *Hemisphere* | *FA m (SD)* | *KFA m (SD)* | *FA m (SD)* | *KFA m (SD)* | *FA m (SD)* | *KFA m (SD)* |
| EF | Anterior thalamic radiation | Left | 0.428 (0.020) | 0.502 (0.024) | 0.428 (0.020) | 0.503 (0.025) | 0.427 (0.019) | 0.500 (0.025) |
| | | Right | 0.421 (0.018) | 0.501 (0.026) | 0.422 (0.020) | 0.501 (0.025) | 0.419 (0.017) | 0.501 (0.027) |
| IS | Fornix | Left | 0.312 (0.039) | 0.307 (0.045) | 0.316 (0.044) | 0.312 (0.052) | 0.309 (0.034) | 0.302 (0.038) |
| | | Right | 0.301 (0.042) | 0.314 (0.049) | 0.320 (0.035) | 0.328 (0.043) | 0.299 (0.046) | 0.300 (0.051) |
| NE | Uncinate fasciculus | Left | 0.415 (0.024) | 0.506 (0.028) | 0.421 (0.024) | 0.510 (0.029) | 0.409 (0.023) | 0.501 (0.026) |
| | | Right | 0.416 (0.024) | 0.507 (0.028) | 0.423 (0.022) | 0.516 (0.027) | 0.408 (0.024) | 0.498 (0.028) |

**Table 4.** Predicting dichotomous relapse based on diffusion metrics measured during early abstinence.

| | | | *FA* | | | *KFA* | | |
|---|---|---|---|---|---|---|---|---|
| *Domain* | *Tract* | *Hemisphere* | *Est.* | *CI* | *p* | *Est.* | *CI* | *p* |
| EF | Anterior thalamic radiation | Left | 1.00 | (0.74–1.36) | 0.996 | 0.96 | (0.74–1.23) | 0.763 |
| | | Right | 1.01 | (0.73–1.40) | 0.975 | 1.04 | (0.81–1.33) | 0.731 |
| IS | Fornix | Left | 0.94 | (0.79–1.11) | 0.462 | 0.93 | (0.80-1.07) | 0.314 |
| | | Right | 0.80 | (0.66–0.95) | 0.018[a] | 0.79 | (0.66–0.92) | **0.006**[b] |
| NE | Uncinate Fasciculus | Left | 0.83 | (0.63–1.08) | 0.178 | 0.85 | (0.66–1.08) | 0.195 |
| | | Right | 0.82 | (0.62–1.06) | 0.140 | 0.82 | (0.64–1.02) | 0.085 |

[a]Significant only before Bonferroni correction [b]Significant after correction for multiple comparisons

**Table 5.** Predicting days-to-relapse based on diffusion metrics measured during early abstinence.

| | | | *FA* | | | *KFA* | | |
|---|---|---|---|---|---|---|---|---|
| *Domain* | *Tract* | *Hemisphere* | *Est.* | *CI* | *p* | *Est.* | *CI* | *p* |
| EF | Anterior thalamic radiation | Left | 0.95 | (0.77–1.17) | 0.628 | 0.94 | (0.79–1.12) | 0.476 |
| | | Right | 0.98 | (0.78–1.23) | 0.861 | 1.02 | (0.86–1.21) | 0.818 |
| IS | Fornix | Left | 0.98 | (0.87–1.10) | 0.707 | 0.96 | (0.88-1.06) | 0.453 |
| | | Right | 0.86 | (0.76–0.96) | 0.011[a] | 0.86 | (0.78–0.95) | **0.002**[b] |
| NE | Uncinate fasciculus | Left | 0.86 | (0.71–1.05) | 0.137 | 0.90 | (0.77–1.05) | 0.170 |
| | | Right | 0.85 | (0.71–1.01) | 0.064 | 0.86 | (0.74–1.01) | 0.062 |

[a]Significant only before Bonferroni correction [b]Significant after correction for multiple comparisons

only domain in which a significant relationship was found with either dichotomous or continuous relapse. These findings align with our prior results based on RSFC strength, where IS domain hypoconnectivity was predictive of both continuous and dichotomous relapse outcomes and was the only domain that remained a significant predictor of dichotomous relapse after controlling for sex (Camchong et al. 2022). Due to its role in the mesolimbic reward pathway, microstructural abnormalities in the fornix may be associated with cue-induced alcohol craving and habit-like compulsive alcohol consumption (Koob and Volkow 2016).

Though not significant, increased FA and KFA in the bilateral UF (NE domain) were associated with decreased odds of continuous and dichotomous relapse in our sample. Microstructural abnormalities in the UF likely influence emotional processing (Von Der Heide et al. 2013) which could exacerbate symptoms of protracted withdrawal in those undergoing treatment for AUD (Koob and Volkow 2016). Although not significant in our limited sample, the directionality and strength of the observed relationship suggest that further exploration of this relationship is merited.

In the IS and NE domains, the direction of all observed relationships was negative, with increases in anisotropy corresponding to decreased risk of relapse and longer periods of sustained abstinence and vice versa. Under the common interpretation of anisotropy as a proxy for white matter integrity, this is the expected directionality and suggests that relapse risk in AUD may be related to white matter that is damaged or underdeveloped. Impaired structural connectivity may also explain our previous observation of decreased RSFC in these domains (Camchong et al. 2022). However, caution must be taken in interpreting diffusion metrics and further exploration of these findings is warranted (see *Considerations*).

## Comparison to prior research

Several previous studies have also investigated white matter microstructure in the context of relapse in AUD. Using a design similar to the present study, Zou et al. (2018) reported decreased FA in the genu and splenium of the corpus callosum as well as the right fornix/stria terminalis in participants who went on to relapse compared to those who remained abstinent. Sorg et al. (2012) also reported lower FA in callosum, bilateral UF, right superior corona radiata, and left anterior internal capsule in participants who returned to heavy use compared to those who abstained as measured six months after treatment. These studies used a whole brain, tract-based spatial statistics (TBSS) approach that substantially differs from our tractography-driven approach. Nonetheless, our observations

in the fornix and UF are broadly consistent with these prior studies.

While the present study focused on white matter microstructure as a predictor of relapse in AUD, it is important to also consider how microstructure is itself impacted by abstinence/relapse. In a relevant longitudinal study, Pfefferbaum et al. (2014) reported that age-related decreases in FA across wide areas of the brain were exaggerated in participants with AUD who relapsed after treatment, while those who abstained showed a flatter trajectory suggesting that FA may recover to normal ranges in prolonged abstinence. Several other studies have also presented evidence that white matter alterations in AUD may be at least partially reversible (Gazdzinski et al. 2010; Alhassoon et al. 2012; Zou et al. 2017).

## Considerations

We relied on a theoretical model of addiction (Koob and Volkow 2010; Koob and Volkow 2016) to inform the a priori selection of several white matter tracts in which we hypothesized that microstructural measures may relate to relapse risk in AUD. In the context of our limited sample size, we lack sufficient power to address the *specificity* of our findings and thus cannot determine whether similar effects may also be found elsewhere in the brain. Furthermore, the theoretical model on which we relied was derived in large part from research on animal models of addiction that may not necessarily extend to AUD in humans. Although this analysis leveraged the Koob–Volkow model in its design, the results should not be interpreted as supporting or refuting the model's validity.

Although diffusion MRI is a useful tool for examining white matter microstructure in vivo, caution must be taken when interpreting how these metrics may reflect the biophysical properties of the underlying tissue (Mueller et al. 2015). A variety of microstructural features may influence the diffusion signal and therefore metrics derived from it, including myelination, axonal damage, and orientation of crossing fibers (De Erausquin and Alba-Ferrara 2013). Our primary goal was to assess whether measurable microstructural alterations were associated with relapse in AUD. The *nature* of those differences is beyond the scope of this study. Furthermore, we are unable to infer from our data whether variations in FA and KFA were caused by chronic alcohol use or if they were pre-existing, perhaps even predisposing individuals to AUD. These questions are well suited for future research.

Interpretation of these findings in relation to our recent report on RSFC in Koob–Volkow domains (Camchong et al. 2022) requires some additional considerations. The white matter tracts chosen to represent each domain in the present study were selected from the 23 expertly defined pathways available in FSL's XTRACT. Perfect correspondence, wherein each pathway connects those structures and *only* those structures that comprised the RSFC networks used in our prior study, was not feasible. Further investigations using alternative tractography approaches may provide additional information. Furthermore, we do not provide direct evidence to determine whether the observed microstructural effects cause resting state hypoconnectivity or instead reflect structural degradation as a result of sustained hypoconnectivity.

## Conclusions

We observed that decreases in anisotropy measures of the right fornix, a white matter tract involved in the IS domain, were related to an increased risk of dichotomous relapse as well as shorter duration of abstinence among individuals with AUD in an inpatient treatment program. No significant relationships between microstructure and relapse outcomes were found in tracts representing the EF and NE domains, but the observed relationship between microstructure and relapse in NE domain tracts (bilateral UF) encourages further exploration using a larger sample. This study supplements our previous report in which reduced RSFC in domain-specific networks was associated with increased relapse risk in AUD. The current findings suggest that some microstructural features may also mediate relapse risk. Further investigation is needed into how the structure and function of these addiction networks may modulate resilience to relapse.

## Funding

This work was supported by the National Institute of Health (K01AA026349 to M.F. and J.C.; UL1TR002494 to J.C.; MH116987 to M.F. and K.O.L.; UG3DA048508 and R01DA038984 to K.O.L.; P41EB027061, P30NS076408, S10OD017974-01 to CMRR) and the Westlake Wells Foundation (to J.C.). The opinions and assertions expressed herein are those of the authors and do not necessarily reflect the official policy or position of the National Institute of Health or the Westlake Wells Foundation. All authors have declared that there are no competing or potential conflicts of interest.

*Conflict of interest statement:* None declared.

## Author contributions

Donovan J. Roediger (Conceptualization, Data curation, Formal analysis, Investigation, Methodology, Visualization, Writing—original draft, Writing—review and editing), Claire Griffin (Conceptualization, Formal analysis, Investigation, Methodology, Project administration, Writing—original draft, Writing—review and editing), Frances V. Marin (Investigation, Project administration, Writing—original draft, Writing—review and editing), Hannah Verdoorn (Data curation, Formal analysis, Investigation, Project administration, Writing—original draft, Writing—review and editing), Mark Fiecas (Formal analysis, Funding acquisition, Methodology, Validation, Writing—review and editing), Bryon A. Mueller (Formal analysis, Methodology, Supervision, Validation, Writing—review and editing), Kelvin O. Lim (Funding acquisition, Project administration, Software, Supervision, Writing—review and editing), Jazmin Camchong (Conceptualization, Data curation, Formal analysis, Funding acquisition, Investigation, Methodology, Project administration, Supervision, Validation, Writing—original draft, Writing—review and editing).

## References

Alfano V, Longarzo M, Aiello M, Soricelli A, Cavaliere C. Cerebral microstructural abnormalities in impulsivity: a magnetic resonance study. *Brain Imaging Behav*. 2021:15(1):346–354. https://doi.org/10.1007/s11682-020-00261-2.

Alhassoon OM, Sorg SF, Taylor MJ, Stephan RA, Schweinsburg BC, Stricker NH, Gongvatana A, Grant I. Callosal white matter microstructural recovery in abstinent alcoholics: a longitudinal diffusion tensor imaging study. *Alcohol Clin Exp Res*. 2012:36(11):1922–1931. https://doi.org/10.1111/j.1530-0277.2012.01808.x.

Andersson JLR, Sotiropoulos SN. An integrated approach to correction for off-resonance effects and subject movement in diffusion MR imaging. *NeuroImage*. 2016:125:1063–1078. https://doi.org/10.1016/j.neuroimage.2015.10.019.

Andersson JLR, Skare S, Ashburner J. How to correct susceptibility distortions in spin-echo echo-planar images: application to diffusion tensor imaging. *NeuroImage*. 2003:20(2):870–888. https://doi.org/10.1016/S1053-8119(03)00336-7.

Andersson JLR, Graham MS, Zsoldos E, Sotiropoulos SN. Incorporating outlier detection and replacement into a non-parametric framework for movement and distortion correction of diffusion MR images. *NeuroImage*. 2016:141:556–572. https://doi.org/10.1016/j.neuroimage.2016.06.058.

Andersson JLR, Graham MS, Drobnjak I, Zhang H, Filippini N, Bastiani M. Towards a comprehensive framework for movement and distortion correction of diffusion MR images: within volume movement. *NeuroImage*. 2017:152:450–466. https://doi.org/10.1016/j.neuroimage.2017.02.085.

Andersson JLR, Graham MS, Drobnjak I, Zhang H, Campbell J. Susceptibility-induced distortion that varies due to motion: correction in diffusion MR without acquiring additional data. *NeuroImage*. 2018:171:277–295. https://doi.org/10.1016/j.neuroimage.2017.12.040.

Beck AT, Steer RA, Carbin MG. Psychometric properties of the Beck Depression Inventory: twenty-five years of evaluation. *Clin Psychol Rev*. 1988:8(1):77–100. https://doi.org/10.1016/0272-7358(88)90050-5.

Brown RJ, Winocur G. The Fornix as a reward pathway. *Physiol Behav*. 1973:11(1):47–52. https://doi.org/10.1016/0031-9384(73)90121-2.

Camchong J, Haynos AF, Hendrickson T, Fiecas MB, Gilmore CS, Mueller BA, Kushner MG, Lim KO. Resting hypoconnectivity of theoretically defined addiction networks during early abstinence predicts subsequent relapse in alcohol use disorder. *Cereb Cortex*. 2022:32(12):2688–2702. https://doi.org/10.1093/cercor/bhab374.

Dale AM, Fischl B, Sereno MI. Cortical surface-based analysis. *I. Segmentation and surface reconstruction. NeuroImage*. 1999:9:179–194. https://doi.org/10.1006/nimg.1998.0395.

Damme KS, Young CB, Nusslock R. Elevated nucleus accumbens structural connectivity associated with proneness to hypomania: a reward hypersensitivity perspective. *Soc Cogn Affect Neurosci*. 2017:12(6):928–936. https://doi.org/10.1093/scan/nsx017.

De Erausquin G, Alba-Ferrara L. What does anisotropy measure? Insights from increased and decreased anisotropy in selective fiber tracts in schizophrenia. *Front Integr Neurosci*. 2013:7:9. https://doi.org/10.3389/fnint.2013.00009.

Deeken F, Banaschewski T, Kluge U, Rapp MA. Risk and protective factors for alcohol use disorders across the lifespan. *Curr Addict Rep*. 2020:7(3):245–251. https://doi.org/10.1007/s40429-020-00313-z.

Dosenbach NUF, Fair DA, Cohen AL, Schlaggar BL, Petersen SE. A dual-networks architecture of top-down control. *Trends Cogn Sci*. 2008:12(3):99–105. https://doi.org/10.1016/j.tics.2008.01.001.

Flannery BA, Volpicelli JR, Pettinati HM. Psychometric properties of the Penn Alcohol Craving Scale. *Alcohol Clin Exp Res*. 1999:23(8):1289–1295.

Gazdzinski S, Durazzo TC, Mon A, Yeh P-H, Meyerhoff DJ. Cerebral white matter recovery in abstinent alcoholics–a multimodality magnetic resonance study. *Brain J Neurol*. 2010:133(Pt 4):1043–1053. https://doi.org/10.1093/brain/awp343.

Glasser MF, Sotiropoulos SN, Wilson JA, Coalson TS, Fischl B, Andersson JL, Xu J, Jbabdi S, Webster M, Polimeni JR, et al. The minimal preprocessing pipelines for the Human Connectome Project. *NeuroImage*. 2013:80:105–124. https://doi.org/10.1016/j.neuroimage.2013.04.127.

Glenn GR, Helpern JA, Tabesh A, Jensen JH. Quantitative assessment of diffusional kurtosis anisotropy. *NMR Biomed*. 2015:28(4):448–459. https://doi.org/10.1002/nbm.3271.

Goldstein RZ, Volkow ND. Dysfunction of the prefrontal cortex in addiction: neuroimaging findings and clinical implications. *Nat Rev Neurosci*. 2011:12(11):652–669. https://doi.org/10.1038/nrn3119.

Grant BF, Goldstein RB, Saha TD, Chou SP, Jung J, Zhang H, Pickering RP, Ruan WJ, Smith SM, Huang B, et al. Epidemiology of DSM-5 alcohol use disorder: results from the National Epidemiologic Survey on alcohol and related conditions III. *JAMA Psychiatry*. 2015:72(8):757–766. https://doi.org/10.1001/jamapsychiatry.2015.0584.

Haddad SMH, Scott CJM, Ozzoude M, Holmes MF, Arnott SR, Nanayakkara ND, Kwan D, Tan B, Casaubon L, Mandzia J, et al. Disintegration of anterior thalamic radiation fibers in cerebrovascular disease subjects with periventricular white matter hyperintensities leads to lower executive function performance. *Alzheimers Dement*. 2021:17(S4):e056596. https://doi.org/10.1002/alz.056596.

Hansen B. An introduction to kurtosis fractional anisotropy. *AJNR Am J Neuroradiol*. 2019:40(10):1638–1641. https://doi.org/10.3174/ajnr.A6235.

Hansen B, Jespersen SN. Kurtosis fractional anisotropy, its contrast and estimation by proxy. *Sci Rep*. 2016:6(1):23999. https://doi.org/10.1038/srep23999.

Jacobus J, Squeglia LM, Bava S, Tapert SF. White matter characterization of adolescent binge drinking with and without co-occurring marijuana use: a 3-year investigation. *Psychiatry Res*. 2013:214(3):374–381. https://doi.org/10.1016/j.pscychresns.2013.07.014.

Jensen JH, Helpern JA. MRI quantification of non-Gaussian water diffusion by kurtosis analysis. *NMR Biomed*. 2010:23(7):698–710. https://doi.org/10.1002/nbm.1518.

Joutsa J, Saunavaara J, Parkkola R, Niemelä S, Kaasinen V. Extensive abnormality of brain white matter integrity in pathological gambling. *Psychiatry Res Neuroimaging*. 2011:194:340–346. https://doi.org/10.1016/j.pscychresns.2011.08.001.

Koob GF, Volkow ND. Neurocircuitry of addiction. *Neuropsychopharmacology*. 2010:35(1):217–238. https://doi.org/10.1038/npp.2009.110.

Koob GF, Volkow ND. Neurobiology of addiction: a neurocircuitry analysis. *Lancet Psychiatry*. 2016:3(8):760–773. https://doi.org/10.1016/S2215-0366(16)00104-8.

Kwako LE, Schwandt ML, Ramchandani VA, Diazgranados N, Koob GF, Volkow ND, Blanco C, Goldman D. Neurofunctional domains derived from deep behavioral phenotyping in alcohol use disorder. *Am J Psychiatry*. 2019:176(9):744–753. https://doi.org/10.1176/appi.ajp.2018.18030357.

Luciana M, Collins PF, Muetzel RL, Lim KO. Effects of alcohol use initiation on brain structure in typically developing adolescents. *Am J Drug Alcohol Abuse*. 2013:39(6):345–355. https://doi.org/10.3109/00952990.2013.837057.

Mamiya PC, Richards TL, Kuhl PK. Right forceps minor and anterior thalamic radiation predict executive function skills in young bilingual adults. *Front Psychol*. 2018:9:118. https://doi.org/10.3389/fpsyg.2018.00118.

McKay JR, Hiller-Sturmhöfel S. Treating alcoholism as a chronic disease. *Alcohol Res Health*. 2011:33(4):356–370.

Monnig MA, Tonigan JS, Yeo RA, Thoma RJ, McCrady BS. White matter volume in alcohol use disorders: a meta-analysis. *Addict Biol*. 2013:18(3):581–592. https://doi.org/10.1111/j.1369-1600.2012.00441.x.

Mueller BA, Lim KO, Hemmy L, Camchong J. Diffusion MRI and its role in neuropsychology. *Neuropsychol Rev*. 2015:25(3):250–271. https://doi.org/10.1007/s11065-015-9291-z.

Niida R, Yamagata B, Niida A, Uechi A, Matsuda H, Mimura M. Aberrant anterior thalamic radiation structure in bipolar disorder: a diffusion tensor tractography study. *Front Psych*. 2018:9:522. https://doi.org/10.3389/fpsyt.2018.00522.

Noble S, Scheinost D, Constable RT. A decade of test-retest reliability of functional connectivity: a systematic review and meta-analysis. *NeuroImage*. 2019:203:116157. https://doi.org/10.1016/j.neuroimage.2019.116157.

Oliva F, Nibbio G, Vizzuso P, Jaretti Sodano A, Ostacoli L, Carletto S, Picci RL. Gender differences in anxiety and depression before and after alcohol detoxification: anxiety and depression as gender-related predictors of relapse. *Eur Addict Res*. 2018:24:163–172. https://doi.org/10.1159/000490046.

Olson IR, Heide RJVD, Alm KH, Vyas G. Development of the uncinate fasciculus: implications for theory and developmental disorders. *Dev Cogn Neurosci*. 2015:14:50–61. https://doi.org/10.1016/j.dcn.2015.06.003.

Ossola P, Gerra MC, Gerra ML, Milano G, Zatti M, Zavan V, Volpi R, Marchesi C, Donnini C, Gerra G, et al. Alcohol use disorders among adult children of alcoholics (ACOAs): gene-environment resilience factors. *Prog Neuro-Psychopharmacol Biol Psychiatry*. 2021:108:110167. https://doi.org/10.1016/j.pnpbp.2020.110167.

Pando-Naude V, Toxto S, Fernandez-Lozano S, Parsons CE, Alcauter S, Garza-Villarreal EA. Gray and white matter morphology in substance use disorders: a neuroimaging systematic review and meta-analysis. *Transl Psychiatry*. 2021:11(1):1–18. https://doi.org/10.1038/s41398-020-01128-2.

Pareaud M, Girard M, Nubukpo P. Factors for maintaining abstinence at 2 and 6 months after alcohol withdrawal. *J Psychiatr Pract*. 2021:27(1):2–13. https://doi.org/10.1097/PRA.0000000000000522.

Pfefferbaum A, Rosenbloom M, Rohlfing T, Sullivan EV. Degradation of association and projection white matter systems in alcoholism detected with quantitative fiber tracking. *Biol Psychiatry*. 2009:65(8):680–690. https://doi.org/10.1016/j.biopsych.2008.10.039.

Pfefferbaum A, Rosenbloom MJ, Chu W, Sassoon SA, Rohlfing T, Pohl KM, Zahr NM, Sullivan EV. White matter microstructural recovery with abstinence and decline with relapse in alcohol dependence interacts with normal ageing: a controlled longitudinal DTI study. *Lancet Psychiatry*. 2014:1(3):202–212. https://doi.org/10.1016/S2215-0366(14)70301-3.

Alcohol Questions and Answers | CDC. 2022. [accessed 2022 Nov 14]. https://www.cdc.gov/alcohol/faqs.htm

Sanchez-Roige S, Baro V, Trick L, Peña-Oliver Y, Stephens DN, Duka T. Exaggerated waiting impulsivity associated with human binge drinking, and high alcohol consumption in mice. *Neuropsychopharmacology*. 2014:39(13):2919–2927. https://doi.org/10.1038/npp.2014.151.

Shin H, Lee S-Y, Cho H-U, Oh Y, Kim IY, Lee KH, Jang DP, Min H-K. Fornix stimulation induces metabolic activity and dopaminergic response in the nucleus accumbens. *Front Neurosci*. 2019:13:1109. https://doi.org/10.3389/fnins.2019.01109.

Sliedrecht W, de Waart R, Witkiewitz K, Roozen HG. Alcohol use disorder relapse factors: a systematic review. *Psychiatry Res*. 2019:278:97–115. https://doi.org/10.1016/j.psychres.2019.05.038.

Smith SM, Jenkinson M, Woolrich MW, Beckmann CF, Behrens TEJ, Johansen-Berg H, Bannister PR, De Luca M, Drobnjak I, Flitney DE, et al. Advances in functional and structural MR image analysis and implementation as FSL. *NeuroImage*. 2004:23(Suppl 1):S208–S219. https://doi.org/10.1016/j.neuroimage.2004.07.051.

Sobell LC, Sobell MB. Timeline follow-back: A technique for assessing self-reported alcohol consumption. In: Litten RZ, Allen JP, editors. *Measuring Alcohol Consumption. Psychosocial and Biochemical Methods*. Totowa, NJ: Humana Press; 1992. p. 41–72. https://doi.org/10.1007/978-1-4612-0357-5_3.

Sorg SF, Taylor MJ, Alhassoon OM, Gongvatana A, Theilmann RJ, Frank LR, Grant I. Frontal white matter integrity predictors of adult alcohol treatment outcome. *Biol Psychiatry*. 2012:71(3):262–268. https://doi.org/10.1016/j.biopsych.2011.09.022.

Spielberger CD, Gorsuch RL, Lushene RE. *STAI manual for the Stait-Trait Anxiety Inventory ("self-evaluation questionnaire")*. Palo Alto, CA: Consulting Psychologists Press; 1970

Stohs ME, Schneekloth TD, Geske JR, Biernacka JM, Karpyak VM. Alcohol craving predicts relapse after residential addiction treatment. *Alcohol Alcohol*. 2019:54(2):167–172. https://doi.org/10.1093/alcalc/agy093.

Tabesh A, Jensen JH, Ardekani BA, Helpern JA. Estimation of tensors and tensor-derived measures in diffusional kurtosis imaging. *Magn Reson Med*. 2011:65(3):823–836. https://doi.org/10.1002/mrm.22655.

Taylor WD, MacFall JR, Gerig G, Krishnan RR. Structural integrity of the uncinate fasciculus in geriatric depression: relationship with age of onset. *Neuropsychiatr Dis Treat*. 2007:3(5):669–674.

Vollstädt-Klein S, Wichert S, Rabinstein J, Bühler M, Klein O, Ende G, Hermann D, Mann K. Initial, habitual and compulsive alcohol use is characterized by a shift of cue processing from ventral to dorsal striatum. *Addict Abingdon Engl*. 2010:105(10):1741–1749. https://doi.org/10.1111/j.1360-0443.2010.03022.x.

Von Der Heide RJ, Skipper LM, Klobusicky E, Olson IR. Dissecting the uncinate fasciculus: disorders, controversies and a hypothesis. *Brain*. 2013:136(6):1692–1707. https://doi.org/10.1093/brain/awt094.

Warrington S, Bryant KL, Khrapitchev AA, Sallet J, Charquero-Ballester M, Douaud G, Jbabdi S, Mars RB, Sotiropoulos SN. XTRACT - standardised protocols for automated tractography in the human and macaque brain. *NeuroImage*. 2020:217:116923. https://doi.org/10.1016/j.neuroimage.2020.116923.

Wong NML, Cheung S-H, Chan CCH, Zeng H, Liu Y-P, So K-F, Lee TMC. Diffusivity of the uncinate fasciculus in heroin users relates to their levels of anxiety. *Transl Psychiatry*. 2015:5(4):e554. https://doi.org/10.1038/tp.2015.48.

Yuan F, Zhu X, Kong L, Shen H, Liao W, Jiang C. White matter integrity deficit associated with betel quid dependence. *Front Psych*. 2017:8:201. https://doi.org/10.3389/fpsyt.2017.00201.

Zhang Y, Wang T, Lei J, Guo S, Wang S, Gu Y, Wang S, Dou Y, Zhuang X. Cerebral damage after carbon monoxide poisoning: a longitudinal diffusional kurtosis imaging study. *Am J Neuroradiol*. 2019:40(10):1630–1637. https://doi.org/10.3174/ajnr.A6201.

Zhou M, Hu Y, Huang R, Zhou Y, Xie X, Zhang S, Jia S, Zhang Y, Xue T, Dong F, et al. Right arcuate fasciculus and left uncinate fasciculus abnormalities in young smoker. *Addict Biol*. 2022:27(2):e13132. https://doi.org/10.1111/adb.13132.

Zou Y, Murray DE, Durazzo TC, Schmidt TP, Murray TA, Meyerhoff DJ. Effects of abstinence and chronic cigarette smoking on white matter microstructure in alcohol dependence: diffusion tensor imaging at 4T. *Drug Alcohol Depend*. 2017:175:42–50. https://doi.org/10.1016/j.drugalcdep.2017.01.032.

Zou Y, Murray DE, Durazzo TC, Schmidt TP, Murray TA, Meyerhoff DJ. White matter microstructural correlates of relapse in alcohol dependence. *Psychiatry Res Neuroimaging*. 2018:281:92–100. https://doi.org/10.1016/j.pscychresns.2018.09.004.